Available online at www.sciencedirect.com
SCIENCE DIRECT
Journal of Power Sources 158 (2006) 730–734
JOURNAL OF POWER SOURCES
www.elsevier.com/locate/jpowsour

Hydrogen absorption and electrochemical properties of Mg_2Ni-type alloys synthesized by mechanical alloying

M.V. Simičić [a,*], M. Zdujić [b], R. Dimitrijević [c], Lj. Nikolić-Bujanović [a], N.H. Popović [a]

[a] *Chemical Power Sources Institute, Belgrade, Serbia and Montenegro*
[b] *Institute of Technical Sciences of the Serbian Academy of Sciences and Arts, Belgrade, Serbia and Montenegro*
[c] *Faculty of Mining and Geology, Department of Crystallography, University of Belgrade, Belgrade, Serbia and Montenegro*

Received 11 November 2004; received in revised form 19 July 2005; accepted 6 September 2005
Available online 21 November 2005

Abstract

Mg_2Ni-type alloys, i.e., Mg_2Ni, $Mg_2Ni_{0.75}Cu_{0.25}$, $Mg_2Ni_{0.6}Cu_{0.4}$ and $Mg_2Ni_{0.75}V_{0.25}$ were synthesized by mechanical alloying and subsequent thermal treatment starting from a corresponding elemental powder mixture. The kinetics of hydrogen absorption and desorption of annealed materials were measured using a manually controlled Sieverts apparatus. The electrochemical characteristics of Mg_2Ni-type alloys were tested for their ability to store hydrogen at room temperature by using constant current to charge and discharge the electrode. The partial substitutions of Cu and V for Ni increased hydrogen absorption and desorption at 200 °C and improved the electrochemical storage capacity and cycle life at room temperature.

Keywords: Mechanical alloying; Mg_2Ni-type alloy; Hydrogen storage

1. Introduction

Magnesium and its alloys are looked upon as one of the most promising hydrogen storage materials owing to their high theoretical storage capacity (up to 3.6 wt.%), light weight and low cost. However, high operating temperatures and slow desorption kinetic prevent their practical application. Extensive research has been focused on the Mg_2Ni-type alloys for use in Ni–MH secondary batteries [1–10].

The specific capacity and hydriding/dehydriding kinetics of hydride electrode materials depend on their chemical composition and crystalline structure [1–12]. A number of reports have shown that the high hydride formation enthalpy of Mg_2Ni is the reason for its low discharge capacity. The partial substitution of some elements (Cu, Fe, V, Cr, Co) for Ni in Mg_2Ni compound decreases the stability of the hydride and makes the desorption reaction easier [6,13]. However, degradation of materials was so high that more than 50% of the maximum electrode capacity was lost within a few cycles. It is well-known that the hydrogen storage material sustains a volume changes during the charge/discharge process giving rise to alloy cracking and pulverizing which, in turn, makes the surface of the material sensitive to oxidation. Also, it has been reported that the partial substitution of foreign elements (V, Ti, Zr), as well as surface modification, could be very effective in preventing the corrosion of materials, hence improving the cycle performance [4,10,14,15].

The preparation of Mg_2Ni-type alloys is not possible through conventional melting processes due to the high vapor pressure of Mg $\{T_m(Mg) = 922\ K, T_b(Mg) = 1380\ K$ and $T_m(Ni) = 1726\ K\}$. When the mechanical alloying process is applied to synthesize these alloys, they show unusual characteristics, such as nanocrystalline structures or an amorphous state, with extended solubility of hydrogen at lower temperatures [1–20]. Mechanical alloying is a milling method used in the preparation of composite, macroscopically homogeneous powder, with extremely fine microstructure, whereby the starting material is a mixture

* Corresponding author.

0378-7753/$ – see front matter © 2005 Elsevier B.V. All rights reserved.
doi:10.1016/j.jpowsour.2005.09.030

of constituent powders of a given composition. The essence of the process is the solid state alloying by repetitive cold welding and fracture of constitutive powder particles. With prolonged milling, various mechanochemical reactions may take place, which in some cases may lead to the formation of intermetallic compounds, typically, with amorphous or nanocrystalline structure [21].

In the present study, Mg_2Ni, $Mg_2Ni_{0.75}Cu_{0.25}$, $Mg_2Ni_{0.6}Cu_{0.4}$ and $Mg_2Ni_{0.75}V_{0.25}$ alloys were prepared by mechanical alloying (MA) and subsequent thermal treatment. Afterwards, the physicochemical and electrochemical characteristics of the materials were investigated.

2. Experimental procedure

Starting materials for mechanical alloying were Mg chips prepared by drilling an ingot ("Bela Stena" – Serbia, 99.9%) and metal powders of Ni (Sigma–Aldrich Chemical Co., 99%, 100 mesh), Cu (Sigma–Aldrich Chemical Co., >99%, 50 mesh) and V (Sigma–Aldrich Chemical Co., 99%, 200 mesh). Powders were weighed to obtain the desired proportion of a starting powder mixture with a total mass of 5 g. A hardened-steel vial with an internal volume of approximately 250 cm^3, charged with 30 hardened-steel balls of a nominal diameter of 13.4 mm was used as a milling medium. The ball-to-powder mass ratio was about 60. Prior to closing the vial, 20 drops of ethanol as a process control agent were added to the powder mixture in order to reduce sticking effect. The vial was sealed with an o-ring, and the cover tightened with four screws.

All handling was done in a glove box filled with purified, dry (humidity <20 ppm) argon. The mechanical alloying was performed in a Fritsch Pulverisette 5 planetary ball-mill. The angular velocity of the supporting disk and vials was 33.2 s^{-1} (317 rpm) and 41.5 s^{-1} (396 rpm), respectively. The estimated milling intensity was 40.8 W, corresponding to 8.2 W g^{-1} [22]. Milling was done for 5 h without any interruption. Subsequently, the powder was enclosed in the quartz tube filled with purified argon and annealed at a temperature of 450 °C for 48 h. The impurity amount, less then 1 wt.% of Fe and Cr was determined by the inductively coupled plasma spectrometry (ICP).

The X-ray powder diffraction (XRD) patterns were recorded on a Philips PW1710 automated diffractometer using a Cu tube operated at 40 kV and 30 mA. The instrument was equipped with a diffracted beam curved graphite monochromator and Xe-filled proportional counter. Diffraction data were collected in the ranges 2θ Bragg angles, 4–90°, counting for 0.4 s (routine identification) and 1.0 s (crystallite size measurements) at 0.02° steps, respectively. A fixed 1° divergence and 0.1 mm receiving slits were used. Silicon powder was used as a standard for calibration of the diffractometer. All XRD measurements were recorded at ambient temperature.

The unit-cell dimensions of annealed alloys were calculated from powder data, by the least square refinement, using the program LSUCRIPC [23]. The hexagonal unit-cell dimensions and $P6_222$ space group found by Hirata [24], were applied as starting parameters for least square procedure. Crystallite size dimensions, i.e., the length of the coherent domains, <*D*>, were determined by using an interactive Windows program for profile fitting and size analysis Winfit [25]. Full-width at half-maximum (FWHM) values of the (2 0 3) peak at Bragg angle $2\theta = 44.95°$ were fitted assuming Gaussian profile of that peak.

The kinetics of hydrogen absorption and desorption of annealed materials were measured using a manually controlled Sieverts apparatus connected to a data acquisition data logger. The hydrogen absorption was conducted at 2.8 MPa and the hydrogen desorption was conducted in a vacuum. Materials were tested at 200 and 300 °C for their hydrogen absorption and desorption properties.

A mixture of 80% powder and 15% graphite was homogenized in a mortar with a pestle, after which a 5% Teflon binder was added. The powder was both a annealed and non-annealed. The electrodes were fabricated by pressing the mixture onto an expanded Ni screen and applying a pressure of 32 MPa. The electrode cycling was carried out in an open cell in 6 M aqueous solution of KOH with a Hg/HgO (6 M KOH) reference electrode. The cut-off voltage was −0.50 V versus reference electrode. Experiments were performed using an EGG 173 (PAR) galvanostat/potenciostat at 12 mAh g^{-1} current densities.

3. Results and discussion

The characteristic XRD patterns of as-milled alloys and after subsequent heat treatment are shown in Figs. 1 and 2. In the case of the binary mixture of Mg and Ni (denoted as Mg_2Ni), the initial powders have not reacted after 5 h of milling. The powder pattern showed a presence of pure Mg and Ni metal phases only. The mechanical alloying of the ternary Cu and V doped mixtures (denoted as $Mg_2Ni_{0.75}Cu_{0.25}$, $Mg_2Ni_{0.6}Cu_{0.4}$ and $Mg_2Ni_{0.75}V_{0.25}$) led to A_2B type structure. The direct formation of intermetallics was surmised from the XRD patterns of the as-prepared powders (Fig. 1) and subsequently proven by the patterns of heat treated samples shown in Fig. 2. Ternary alloys synthesized by mechanical alloying (Fig. 1), were strongly disordered and nanostructured, but they are free of amorphous phase.

The nanocrystalline nature of alloys obtained after milling is confirmed by crystallite size $<D_{hkl}>$(Å) results presented in Table 1. It is important to notice that <*D*> values were calculated on the same peak having Miller indices (2 0 3) due to better possibility of mutual comparison. The crystallite sizes of alloy particles obtained by milling were between 5 and 10 nm, consistent with results published by other authors [17]. After being heated at 450 °C for 48 h, mechanically alloyed samples passed throughout structure transformation to A_2B type (mechanically alloyed binary Mg–Ni mixture) or structure ordering and growth to bigger crystal blocks, abandoning nanostructured state (ternary mixtures) Table 1. In that way, all treated alloys show well-crystallized XRD patterns (Fig. 2), having A_2B type structure. Additionally, their unit-cell dimension values (Table 1) confirmed the synthesis of A_2B type alloys.

The annealed powders of Mg_2Ni-type alloys were tested at 200 and 300 °C for their hydrogen absorption and desorption properties. The kinetics of hydrogenation were extremely fast, especially at 300 °C (Fig. 3). At 300 °C, the alloys absorbed more than 95% of their hydrogen capacities within the first 5 min

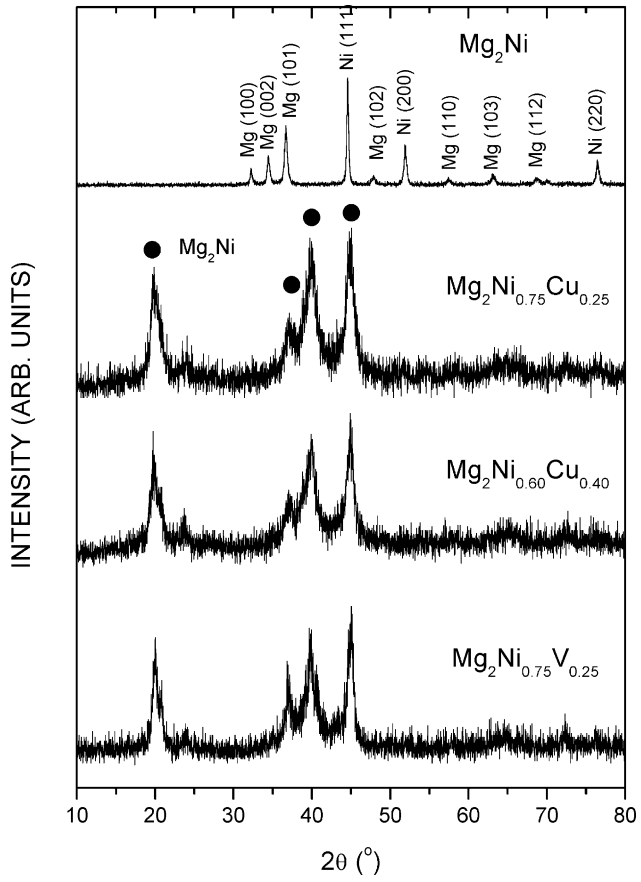

Fig. 1. XRD patterns of Mg_2Ni, $Mg_2Ni_{0.75}Cu_{0.25}$, $Mg_2Ni_{0.6}Cu_{0.4}$ and $Mg_2Ni_{0.75}V_{0.25}$ powder mixtures mechanically alloyed for 5 h (full circles denote characteristic peaks of the Mg_2Ni phase).

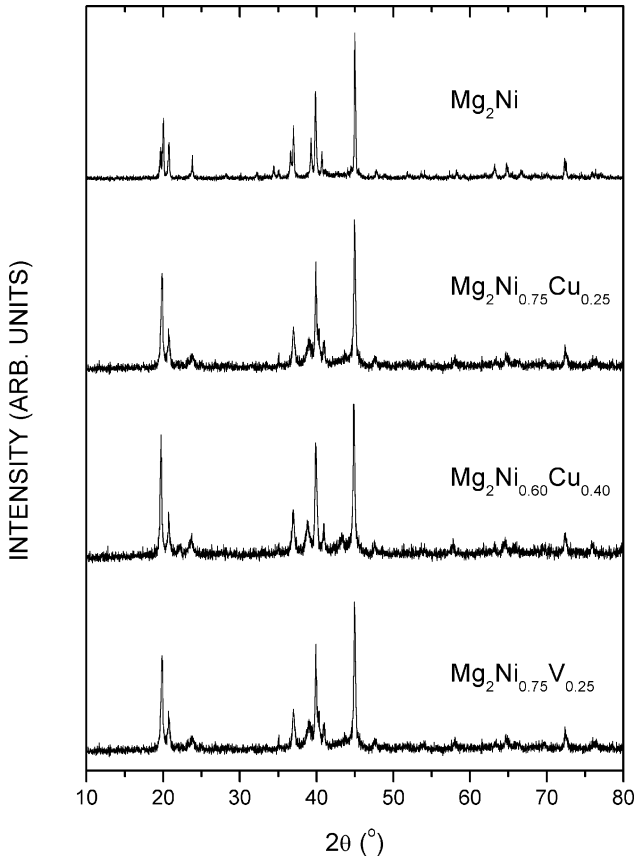

Fig. 2. XRD patterns of Mg_2Ni, $Mg_2Ni_{0.75}Cu_{0.25}$, $Mg_2Ni_{0.6}Cu_{0.4}$ and $Mg_2Ni_{0.75}V_{0.25}$ powder mixtures mechanically alloyed for 5 h were subsequently heated at 450 °C for 48 h.

(Fig. 3). It can be clearly seen that the hydrogen storage capacity of $Mg_2Ni_{0.75}Cu_{0.25}$ alloy at 300 °C was higher (3.76 wt.%) than the hydrogen storage capacity of the others. Absorption kinetics was not found to be extremely sensitive to alloying elements and particle size. Fig. 4 shows that Mg_2Ni-type alloys can desorb a large amount of hydrogen. The maximum hydrogen desorption capacity at 200 °C was $Mg_2Ni_{0.75}Cu_{0.25}$ alloy (2 wt.%). The amount of desorbed hydrogen and kinetics of dehydrogenation were increased by partial substitution of Cu and V for Ni. This effect is attributed to reduction hydride formation enthalpy.

Fig. 5 shows the variation in the discharge capacity of electrodes based on non-annealed Mg_2Ni-type alloys with the cycle number at room temperature. The Mg_2Ni-type alloys milled for 5 h displayed the maximum discharge capacity in the first cycle but degraded strongly with cycling, especially Mg_2Ni sample. The partial substitution of Cu and V for Ni increased the initial discharge capacities of these nanocrystalline alloys and their cycle performance. The rapid degradation could have been caused by the severe corrosion of Mg in the alkaline KOH solution accompanied by the $Mg(OH)_2$ formation on the alloy surface. Especially, during the discharging process, the alloys are anodically polarized so that corrosion would be faster. The maximum discharge capacity of the electrode, which was produced of the $Mg_2Ni_{0.75}Cu_{0.25}$ alloy was 372 mAh g^{-1} in the first cycle.

The variation in the discharge capacity of the electrodes based on 48 h annealed Mg_2Ni-type alloys, with cycle number at room temperature, is shown in Fig. 6. The electrode prepared from

Table 1
The unit-cell parameters and relevant crystallite size of synthesized Mg_2Ni-type alloys

Alloy composition	Ball-milled for 5 h	Subsequently heat treated at 450 °C for 48 h			
	Crystallite size, $<D_{203}>$ (Å)	Crystallite size, $<D_{203}>$ (Å)	Unit-cell parameters		Unit-cell volume
			a (Å)	c (Å)	V (Å^3)
Mg_2Ni	–	1250	5.219(1)	13.293(1)	313.6(2)
$Mg_2Ni_{0.75}Cu_{0.25}$	59	410	5.215(4)	13.18(3)	310.5(6)
$Mg_2Ni_{0.60}Cu_{0.40}$	52	496	5.211(4)	13.24(2)	311.4(6)
$Mg_2Ni_{0.75}V_{0.25}$	102	402	5.227(5)	13.18(4)	312(1)

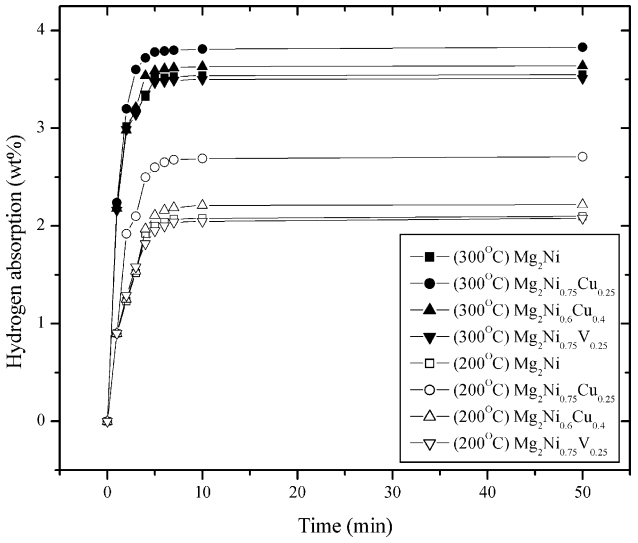

Fig. 3. Hydrogen absorption of the Mg_2Ni-type alloys.

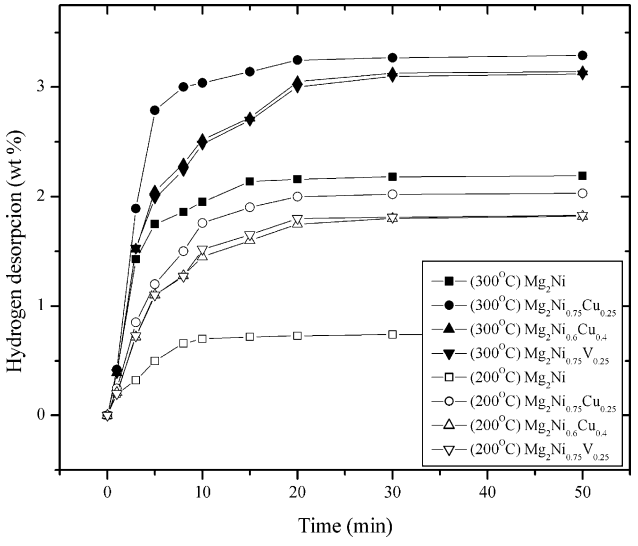

Fig. 4. Hydrogen desorption of the Mg_2Ni-type alloys.

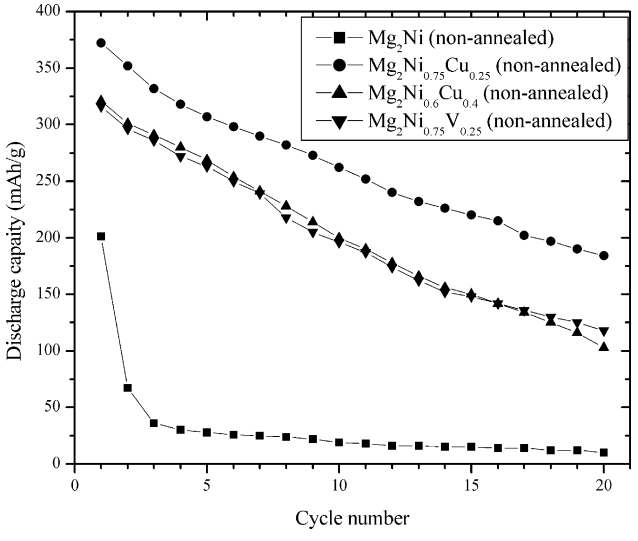

Fig. 5. Discharge capacity variation of the electrodes based on non-annealed Mg_2Ni-type alloys with the cycle number.

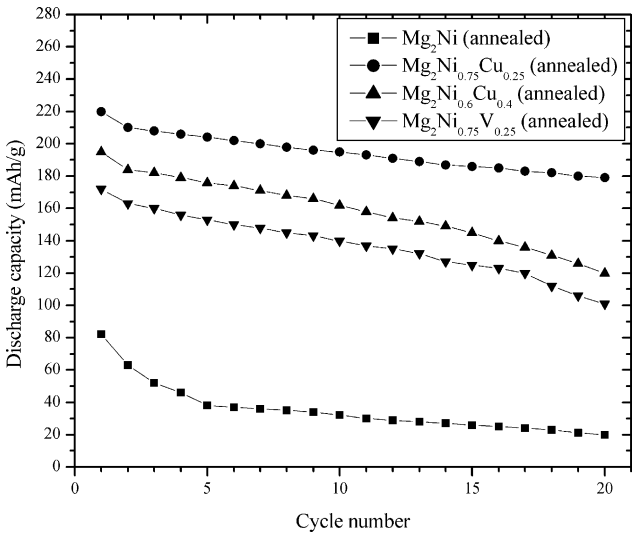

Fig. 6. Discharge capacity variation of the electrodes based on annealed Mg_2Ni-type alloys with the cycle number.

the annealed $Mg_2Ni_{0.75}Cu_{0.25}$ alloy had the highest discharge capacity of 221 mAh g^{-1}.

The effect of crystallite size on electrochemical properties can be seen by comparing Figs. 5 and 6. Annealed alloys consisting of bigger crystal blocks showed significant lower discharge capacities in the first cycle and also lower capacity decays compared to the as-milled nanostructured alloys. The increased discharge capacity of nanocrystalline alloys is related to their large grain boundary area and enhanced charge transfer reaction rate and hydrogen diffusion into hydrogenation sites. However, even if the large grain boundary area of the nanostructured phase was superior for hydrogenation, it was detrimental for corrosion in the electrolyte during cycling. We presume that the improved performance in the cycle life of substituted alloy electrodes is caused by preferential oxidation of Cu and V on the alloy surface and the prevention of the formation of the $Mg(OH)_2$ passive layer.

4. Conclusion

Starting from elemental powders, nanostructured Mg_2Ni-type alloys were prepared by milling for 5 h in a planetary ball-mill. The mechanical alloying of ternary systems, i.e., $Mg_2Ni_{0.75}Cu_{0.25}$, $Mg_2Ni_{0.6}Cu_{0.4}$ and $Mg_2Ni_{0.75}V_{0.25}$ leads to the direct synthesis of nanocrystalline A_2B alloys (crystallite sizes from 6 to 10 nm) with virtually no presence of starting elements. After being heated at 450 °C for 48 h, mechanically alloyed samples passed throughout structure transformation to A_2B type (i.e., mechanically alloyed binary Mg–Ni mixture) or structure, ordering and growing into bigger crystal blocks, abandoning nanostructured state (i.e., ternary mixtures). It was found that the partial substitution of Cu and V for Ni increased hydrogen desorbability at 200 °C and improved electrochemical and cycle performances at room temperature in comparison with Mg_2Ni.

In summary, it can be concluded that the combination of partial substitution and the suitable structural irregularities result-

ing from the ball-milling process improved the performance of Mg_2Ni-type alloys.

Acknowledgments

This study was supported by the Technology Research Fund of the Ministry of Science and Ecology of the Republic of Serbia.

References

[1] S.S. Han, N.H. Goo, W.T. Jeong, K.S. Lee, J. Power Sources 92 (2001) 157.
[2] S. Bouaricha, J.P. Dodelet, D. Guay, J. Huot, S. Boily, R. Schulz, J. Alloys Compd. 307 (2000) 226.
[3] A. Zaluska, L. Zaluski, J.O. Ström-Olsen, J. Alloys Compd. 289 (1999) 197.
[4] N.H. Goo, W.T. Jeong, K.S. Lee, J. Power Sources 87 (2000) 118.
[5] J.H. Woo, C.B. Jung, J.H. Lee, K.S. Lee, J. Alloys Compd. 293–295 (1999) 556.
[6] J.H. Woo, K.S. Lee, J. Electrochem. Soc. 146 (1999) 819.
[7] S.S. Han, H.T. Lee, N.H. Goo, W.T. Jeong, K.S. Lee, J. Alloys Compd. 330–332 (2002) 841.
[8] T. Kuji, H. Nakano, T. Aizawa, J. Alloys Compd. 330–336 (2002) 590.
[9] N.H. Goo, J.H. Woo, K.S. Lee, J. Alloys Compd. 288 (1999) 286.
[10] H.Y. Lee, N.H. Goo, W.T. Jeong, K.S. Lee, J. Alloys Compd. 313 (2000) 258.
[11] A. Zaluska, L. Zaluski, J.O. Ström-Olsen, Appl. Phys. A 72 (2001) 157.
[12] G. Mulas, L. Schiffini, G. Cocco, J. Mater. Res. 19 (2004) 3279.
[13] Y. Takahashi, H. Yukawa, M. Morinaga, J. Alloys Compd. 242 (196) 98.
[14] C. Iwakura, H. Inoue, S. Nohara, R. Shin-ya, S. Kurosaka, K. Miyanohara, J. Alloys Compd. 330–332 (2002) 636.
[15] H.Y. Lee, N.H. Goo, W.T. Jeong, K.S. Lee, J. Alloys Compd. 293–295 (1999) 556.
[16] P. Solsona, S. Doppiu, T. Spassov, S. Suriñach, M.D. Baró, J. Alloys Compd. 381 (2004) 66.
[17] T. Spassov, P. Solsona, S. Suriñach, M.D. Baró, J. Alloys Compd. 349 (2003) 242.
[18] T. Spassov, P. Solsona, S. Bliznakov, S. Suriñach, M.D. Baró, J. Alloys Compd. 356–357 (2003) 639.
[19] J.S. Kim, C.R. Lee, J.W. Choi, S.G. Kang, J. Power Sources 104 (2002) 201.
[20] A.A. Mohamad, N.S. Mohamed, Y. Alias, A.K. Arof, J. Power Sources 115 (2003) 161.
[21] C. Suryanarayana, Prog. Mater. Sci. 46 (2001) 1.
[22] A. Iasonna, M. Magini, Acta Mater. 44 (1996) 1109.
[23] R.G. Garvey, Powder Diff. 1 (1986) 114.
[24] JCPDS card 35-1225.
[25] S. Krumm, Mater. Sci. Forum 228–231 (1996) 183.